

# A Numerical Study of Ultrametricity in Finite Dimensional Spin Glasses

A. Cacciuto, E. Marinari

*Dipartimento di Fisica and Infn, Università di Cagliari  
Via Ospedale 72, 09100 Cagliari (Italy)*

G. Parisi

*Dipartimento di Fisica and Infn, Università di Roma La Sapienza  
P. A. Moro 2, 00185 Roma (Italy)  
(July 3, 2021)*

We use a constrained Monte Carlo technique to analyze ultrametric features of a 4 dimensional Edwards-Anderson spin glass with quenched couplings  $J = \pm 1$ . We find that in the large volume limit an ultrametric structure emerges quite clearly in the overlap of typical equilibrium configurations.

The hierarchical solution [1] of mean field spin glasses [2] introduces a large number of new features. For  $T < T_{SG}$ , in the broken phase, there are many stable equilibrium states, not related by a simple symmetry group (like  $Z_2$  in the normal Ising model). These states exhibit an ultrametric structure: their distance satisfies an inequality stronger than the triangular inequality,  $d_{1,3} \leq d_{1,2} + d_{2,3}$ , the ultrametric inequality, stating that  $d_{1,3} \leq \max(d_{1,2}, d_{2,3})$ . The existence of a phase transition even in non-zero magnetic field (de Almeida-Thouless line) and of a complex dynamics, with aging phenomena, are other crucial features of this picture.

The question of main interest is how many of such remarkable and new features survive the descent to finite dimension. Mean field is in the case of usual, non-disordered systems, giving very good hints about the finite dimensional case, but what about systems which offer such a series of completely new phenomena? In the last period much activity has been devoted to try and clarify this problem. As in many murky situations Monte Carlo simulations are playing an important role [3]. Computing corrections to the field theory of the problem is also a difficult task, but progresses are being obtained [4]. Here in the following we will select the problem of ultrametricity, and try to understand how this feature is modified when going from mean field to finite dimensional, realistic systems.

The hierarchical solution of mean field spin glasses admits a state structure endowed with an ultrametric distance [5] (for a very good discussion of the problem, both introductory and going deep in the details of the subject, see [6]). Distances among states obey the ultrametric inequality we have given before. Let us consider two spin configurations representative of two given states [7]. One can define the squared distance of two spin configurations as

$$d_{\alpha,\beta}^2 \equiv \frac{1}{4q_{EA}V} \sum_{i=1}^V (m_i^\alpha - m_i^\beta)^2 = \frac{1}{2} \left(1 - \frac{q_{\alpha,\beta}}{q_{EA}}\right), \quad (1)$$

where  $q_{\alpha,\beta} \equiv \frac{1}{V} \sum_{i=1}^V \sigma_i^\alpha \sigma_i^\beta$  is the overlap of the two configurations  $C_\alpha$  and  $C_\beta$ . Such  $d^2$  takes the value 0 when the mutual overlap is exactly  $q_{EA}$  (the overlap of two configurations in the same state, i.e. the maximum allowed overlap), and the value 1 when the overlap is  $-q_{EA}$ . This is the distance we will always have in mind in this note.

The main result one obtains in mean field concerns the disorder averaged probability distribution for the probability distribution of three overlaps. We consider three equilibrium configurations, 1, 2 and 3 of the spin systems (interacting by the same given realization of the quenched couplings).  $q_{1,2}$ ,  $q_{2,3}$  and  $q_{1,3}$  are the mutual overlaps. By using the formalism of replica symmetry breaking one finds [5] that

$$\begin{aligned} & \overline{P_J(q_{1,2}, q_{2,3}, q_{1,3})} \\ &= \frac{1}{2} P(q_{1,2}) x(q_{1,2}) \delta(q_{1,2} - q_{2,3}) \delta(q_{1,2} - q_{1,3}) \\ &+ \left\{ \frac{1}{2} \{ P(q_{1,2}) P(q_{2,3}) \theta(q_{1,2} - q_{2,3}) \delta(q_{2,3} - q_{1,3}) \right. \\ &+ \text{two permutations} \} , \end{aligned} \quad (2)$$

where  $x(q) \equiv \int_0^q P(q') dq'$  gives the weight of equilateral triangles (the other three terms represent triangles with the two equal edges longer than the different one).

Further work on the ultrametric features of mean field solution [8] has clarified the robustness of the ultrametric behavior. Numerical work on the subject is contained in references [9,10].

We want to understand what happen in the case of finite dimensional systems. It is clear that the problem is a difficult one: finite size effects are known to be severe, and the use of a scaling analysis is mandatory.

We have used a *constrained Monte Carlo* procedure. For each realization of the quenched disordered couplings we have considered three configurations of the spin variables, say  $C_\alpha$ ,  $C_\beta$  and  $C_\gamma$ . We have fixed the distance of  $C_\alpha$  from  $C_\beta$  and of  $C_\beta$  from  $C_\gamma$  i.e. we have kept fixed to a constant value the overlaps  $q_{\alpha,\beta} \equiv q_{1,2}$  and  $q_{\beta,\gamma} = q_{2,3}$ . A sensible choice of  $q_{1,2}$  and  $q_{2,3}$  is crucial for the method to give useful results. The values  $q_{1,2}$  and  $q_{2,3}$  have been kept constant by forbidding spin updates that bring the overlap  $q_{\alpha,\beta}$  out of the range  $q_{1,2} \pm \epsilon$  or the overlap  $q_{\beta,\gamma}$  out of the range  $q_{2,3} \pm \epsilon$ . For all the simulations discussed in this note we have used  $\epsilon = 0.04$ . A systematic study of the choice of an optimal value for  $\epsilon$  is contained in [11].

By using this procedure we are restricting the phase space: our numerical simulations do not investigate the equilibrium properties of the full model, but only the sector where in a triple of states two distance are fixed. To make the procedure consistent  $q_{1,2}$  and  $q_{2,3}$  have to be chosen in the support of the  $P(q)$  of the full model. A good choice of the constrained value will make the ultrametric bound very different from the triangular bound, making the difference among the two phase space structure as clear as possible.

We have studied the 4 dimensional Edwards-Anderson model, with quenched couplings  $J = \pm 1$  with probability  $\frac{1}{2}$ . The Hamiltonian  $H = \sum_{i,j} \sigma_i J_{ij} \sigma_j$  contains a sum over first neighbors. We have chosen the  $4d$  (as opposite to  $3d$ ) case because here we have a better understanding of the critical behavior [10,3] ( $d = 4$  is farer from the lower critical dimension, and the critical behavior is clearer). We have been working at  $T = 1.4$ , i.e.  $T \simeq 0.7T_c$ , where we are already in the broken phase and the  $P(q)$  has a clear non-trivial structure, but we are still able to completely thermalize the non-constrained system, at least on small lattices [11].

We have used lattices of volume  $V = L^4$  with  $L = 3, 4, 5, 6, 7$  and  $8$ .  $L = 8$  was the maximum lattice size we felt sure we were able to thermalize. We have averaged the  $P_J(q)$  over different realizations of the quenched disordered couplings  $J$ ; in both the numerical experiments we will describe in the following the number of samples  $N_J$  has been a maximum of 2000 for the smallest lattice ( $L = 3$ ) and a minimum of 100 for the largest lattice,  $L = 8$  (with intermediate  $N_J$  values for the intermediate lattice sizes).

We will give more details about the thermalization of the samples, that is for this kind of numerical experiment a crucial issue. We have been very careful about this point, and all the data we present here have passed detailed thermalization tests [11]. For all lattice size we have used an annealing schedule; starting from a random configuration we have cooled the systems from  $T = 2.4$  down to  $T = 1.4$  at steps  $\Delta T = 0.1$  (for the smaller  $L$  values) or  $0.2$  (for the larger ones). At each  $T$  value we have ran from 25000 sweeps ( $L = 3$ ) to 80000 sweeps ( $L = 8$ ). Once at  $T = 1.4$ , after the usual thermalization steps, we have ran from half a million ( $L = 3$ ) to eight hundred thousand sweeps ( $L = 8$ ) for measuring.

Our main results have been obtained by fixing

$$q_{\alpha,\beta} \equiv q_{1,2} = q_{\beta,\gamma} = \frac{2}{5}q_{EA} \equiv \bar{q} , \quad (3)$$

where by  $q_{EA}$  we mean the infinite volume values as estimated for example in [10] (.54). That means we are fixing  $\bar{q} = .21$  for all the volume values we investigate. In this condition the triangular inequality obliges the measured  $q$ , the third side of the triangle, to obey

$$q \geq -\frac{7}{5}q_{EA} , \quad (4)$$

while an ultrametric distance would imply

$$q \geq \frac{2}{5}q_{EA} . \quad (5)$$

It is clear that the two bounds are very different. Obviously in both cases in the infinite volume limit the measured  $q$  will be smaller than  $q_{EA}$ .

In fig. (1) the vertical line on the left, at  $q \simeq -0.75$ , depicts the bound given from the triangular inequality.

The second vertical line, at  $q \simeq .21$ , depicts the ultrametric bound, while the vertical line on the right, at  $q_{EA}$ , is the upper bound for infinite volume. The probability distributions of the measured  $q$  value (the overlap among configuration  $C_\alpha$  and configuration  $C_\beta$ , see before) for the 6  $L$  values, from  $L = 3$  to  $L = 8$ . The  $L = 3$   $P(q)$  is the one with the smaller peak, farthest on the right, that end last on the left:  $P(q)$  for increasing  $L$  values have higher peaks, and end more and more at  $q$  values close to zero. It is clear that already on small lattices the distribution is far from the triangular bound.

The probability for a measured distance  $q$  not to be ultrametric (i.e. one minus the normalized area  $S^U$  of the  $P(q)$  integrated inside the ultrametric bound) decreases fast with the lattice size. On a  $L = 8$  lattice half of the configurations are ultrametric (and indeed the big violation is from configurations with  $q > q_{EA}$ , which we expect from normal Monte Carlo runs to disappear in the continuum limit).

In fig. (2) we plot the value of the integral

$$I^L \equiv \int_{-1}^{q_{min}} (q(L) - q_{min})^2 P(q) dq + \int_{q_{MAX}}^1 (q(L) - q_{MAX})^2 P(q) dq, \quad (6)$$

in log-log scale. Here  $q_{min} = q_{1,2}$  and  $q_{MAX} = q_{EA}$ . The lower points ( $I_1$ ) are for the case we are discussing here, the upper ones for the case where we fix  $q_{1,2} \neq q_{2,3}$  (see later). The straight line is our very good best fit to a power behavior, that gives

$$I^L \simeq (-.0001 \pm .0005) + (0.76 \pm 0.03)L^{-2.21 \pm 0.04}. \quad (7)$$

The integral goes to zero in the infinite volume limit, as we would expect for an ultrametric structure. It is remarkable that the asymptotic value is estimated to be so close to zero, and that the estimated exponent is very close to the  $\frac{8}{3}$  one expects from the results of [8].

A few comments are in order. There are two different and important effects in fig. (1). On the one side the number of configurations with large  $q$  ( $q > q_{EA}^{V=\infty}$ ) decreases with increasing  $L$ . These are the kind of finite size effects that normally one studies. Such finite size effects are already known to be quite large in quenched disordered systems: even for the SK model it is quite difficult to get a good numerical determination of the position of the peak of  $P(q)$  in the infinite volume limit. We confirm that in our simulation. On the other side ( $q < 0$ ) things are different. Already on a very small lattice very few configurations are allowed in the region that is allowed by the triangular inequality but ultrametrically forbidden. This region is systematically reduced when increasing the lattice size (it is basically halved when going from  $L = 3$  to  $L = 8$ ).

We have also fitted the position of the peak of  $P(q)$ ,  $q_{MAX}^{(\infty)}$  with an  $L$ -dependent power law. Our best fit is very good and gives

$$q_{MAX}^{(L)} = (0.31 \pm 0.09) + (0.85 \pm 0.03)L^{-0.59 \pm 0.15}, \quad (8)$$

with a value of  $q_{MAX}^{(\infty)}$  just in the center of the allowed ultrametric region.

These results look very positive. Already on the lattice sizes one can equilibrate with a numerical simulation (in a sector of the phase space) that took a few months of workstation time one clearly sees the increasing domination of ultrametric sample couples. Obviously we do not know if in the infinite volume limit there will be a completely ultrametric structure (we do not have a priori reasons to be sure of that) or if ultrametricity will be realized on finite dimensional spin glasses only as a dominance of states close to ultrametric behavior: certainly, we are showing here that the ultrametric sector of the phase space is very important.

Maybe the most important problem we are detecting is the one of large finite size effects. That was already known, and we confirm it here: for example  $q_{EA}^{(L)}$  converges only very slowly to  $q_{MAX}^{(\infty)}$ .

Thermalization is a key problem. In a constrained dynamics like the one we are using is very difficult to ascertain thermalization. The usual criterion of checking that the dynamical  $P_d(q)$  (i.e. the one where the overlap is defined from  $\lim_{t_1 \rightarrow \infty} \sigma(t)\sigma(t+t_1)$ ) should coincide with the equal time  $P_e(q)$  (where the overlap is from the evolution of two different systems, i.e. from  $\sigma(t)\tau(t)$ ) is not useful here (since in our constrained Monte Carlo method we do not have an equivalent dynamical quantity  $P_d(q)$  to compare with). Also the symmetry  $\sigma \rightarrow -\sigma$  is not a good symmetry here, and the symmetry of  $P(q)$  cannot be used to check thermalization. Because of that we have tried to stay on the very safe side. In figure (3) we plot  $P(q)$  for  $L = 5$  (100 samples) for the first, the second and the third third of the MC sweeps (after the annealing schedule). The three curves are basically identical, making us confident that we are having no thermalization problems.

We have also analyzed a different situation, in which we have set  $q_{1,2} \neq q_{2,3}$ . In this case we have used runs of length similar to the one of the previous case, a similar number of samples, same  $L$  values and  $T = 1.4$ . We have fixed  $q_{1,2} = \frac{4}{5}q_{EA}$  and  $q_{2,3} = \frac{1}{5}q_{EA}$ . In this case an ultrametric behavior implies that in the infinite volume limit  $P(q) = \delta(q - \frac{1}{5}q_{EA})$ , centered in  $\frac{1}{5}q_{EA} \simeq 0.10$ . We report in fig. (4) the  $P(q)$  for this situation. A power fit for the position of the peak in the infinite volume limit gives as a preferred value  $q_{MAX}^{(\infty)} = (0.10 \pm 0.03)$ , right on the ultrametric point. Also in this case we are getting a strong indication toward the presence of ultrametric features in the state space of finite dimensional spin glasses.

In fig. (2) we also plot the value of the integral  $I^L$  for this second case ( $I_2$ ). Here  $q_{min} = q_{MAX}$  is the location where we expect a delta function to be built in the infinite volume limit, and the integral just goes from  $-1$  to  $1$ . The straight line is again the best fit to a power behavior, that gives

$$I^L \simeq (-.000 \pm .002) + (1.95 \pm 0.08)L^{-1.95 \pm 0.04} . \quad (9)$$

Also here the integral seems to be going to zero in the infinite volume limit.

We are grateful to Felix Ritort for sharing with us some ideas about this problem. We also thank Peter Young for an interesting conversation.

- [1] G. Parisi, Phys. Rev. Lett. **43**, 1754 (1979); J. Phys. A **13**, 1101 (1980); **13**, 1887 (1980); **13**, L115 (1980); Phys. Rev. Lett. **50**, 1946 (1983).
- [2] M. Mezard, G. Parisi and M. Virasoro, *Spin Glass Theory and Beyond* (World Scientific, Singapore 1987).
- [3] E. Marinari, G. Parisi, F. Ritort, J. Phys. A **27**, 2687 (1994); E. Marinari, G. Parisi, F. Ritort and J. Ruiz-Lorenzo, Phys. Rev. Lett. **76**, 843 (1996); N. Kawashima and P. Young, cond-mat/9510009.
- [4] See for example C. de Dominicis and I. Kondor, Int. J. Mod. Phys. **B 7** (1993) 986. M. Ferrero and G. Parisi, cond-mat/9511049; P. Ranieri J. Phys. I (France) **6**, 807 (1996), and references therein.
- [5] M. Mezard, G. Parisi, N. Sourlas, G. Toulouse and M. A. Virasoro, Phys. Rev. Lett. **52**, 1156 (1984); J. Phys. (Paris) **45**, 843 (1984).
- [6] R. Rammal, G. Toulouse and M. Virasoro, Rev. Mod. Phys. **58**, 765 (1986).
- [7] G. Parisi, J. Stat. Phys. **72**, 857 (1993).
- [8] S. Franz, G. Parisi and M. A. Virasoro, Europhys. Lett. **17**, 5 (1992); J. Phys. I France **2**, 1869 (1992).
- [9] N. Sourlas, J. Phys. Lett. **45**, L969 (1984); N. Parga, G. Parisi and M. Virasoro, J. Phys. Lett. **45**, L1063 (1984); S. Kirkpatrick and G. Toulouse, J. Phys. **46**, 1277 (1985); R. N. Bhatt and A. P. Young, J. Magn. Mater. **54-57**, 191 (1986).
- [10] J. C. Ciria, G. Parisi and F. Ritort, J. Phys. A: Math. Gen. **26**, 6731 (1993).
- [11] A. Cacciuto, to be published.

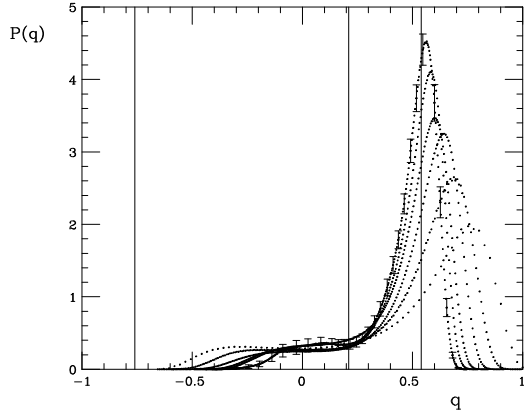


FIG. 1.  $P(q)$  of the free overlap measured in the course of our constrained Monte Carlo as a function of  $q$ , for  $L$  values going from 3 (lowest curve, ending on the left closest to  $q = 0$ ) to  $L = 8$  (highest curve, ending on the left farrest from  $q = 0$ ).

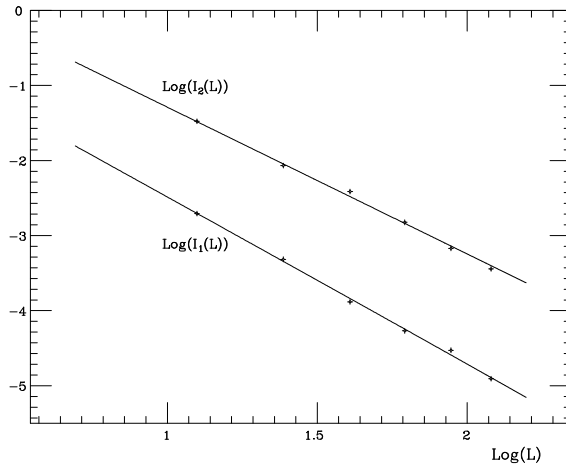


FIG. 2. The integral  $I^L$  as a function of  $L$ , in double log scale. The lower points are for the case where we have fixed  $q_{1,2} = q_{2,3}$ , the upper points where  $q_{1,2} \neq q_{2,3}$  (see the text).

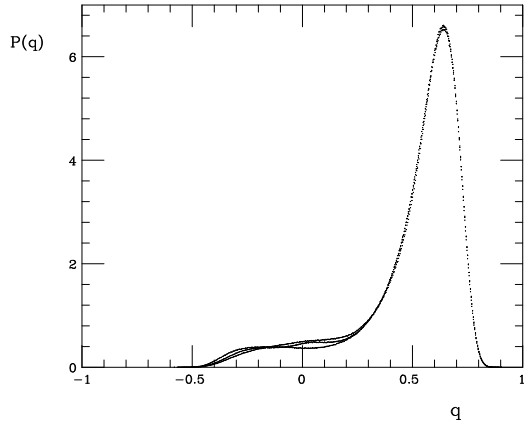


FIG. 3. The three curves (basically coinciding in the plot) are for  $P(q)$  in the first, the second and the last third of the run (after the annealing scheme described in the text),  $L = 5$ , 100 samples.

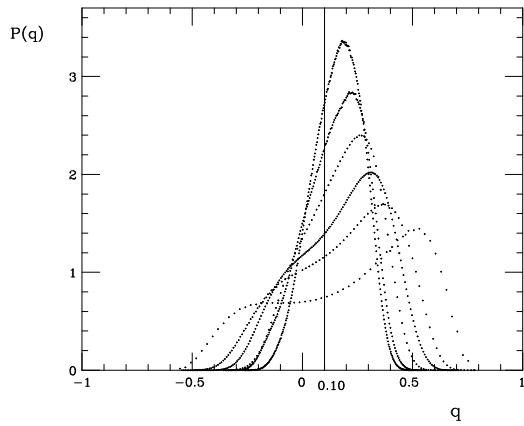


FIG. 4. As in figure (1), but for  $q_{1,2} = \frac{4}{5}q_{EA}$  and  $q_{2,3} = \frac{1}{5}q_{EA}$ .